# A Multiple Interferometer for Analyzing the Vibrations of a Quartz Plate

H. OSTERBERG, *Department of Physics, University of Wisconsin*
(Received March 23, 1933)

A multiple interferometer, by means of which the various types of vibrations in piezoelectric plates can be determined with a certainty far greater than has hitherto been afforded by other methods, is described and illustrated. This interferometer combines in a convenient form six interferometers for measuring the relative motion of any two plane surfaces of the vibrating plate. A simple analysis of the measurement reveals the type of vibration. The application of this interferometer to the study of rectangular quartz plates is illustrated by photographs from two interesting and enlightening patterns appearing in a square plate of $X$-cut. These patterns have previously been studied by R. B. Wright and D. W. Stuart with the aid of lycopodium powder. They appear to be formed by two compressional wave trains propagated in opposite directions in the plane of the plate and incident at angles much different from 90° upon the crystal boundaries. The directions of maximum and minimum outward displacement of the end faces are often those in which Young's modulus assumes a critical value. The actual form of these patterns is undoubtedly affected by the anisotropy of Young's modulus. Efforts to determine the above wave trains with the aid of Huyghen's construction have not yet been successful. However, it appears that this construction is capable of explaining why simple longitudinal patterns, of the open ended organ pipe variety, have never been observed by the writer in the ordinary $X$-cuts.

## INTRODUCTION

IT is well known that a plate possessing piezoelectric properties may be caused to vibrate in a variety of modes by applying to the plate in a suitable manner an alternating voltage of appropriate frequency. Much reliable information about the displacements in these modes can be gained with the aid of a simple interferometer in which interference fringes are formed by reflection from the plane quartz surface under observation and an auxiliary surface of glass. The pattern of nodes and antinodes for the component of displacement normal to the surface is made directly visible. The corresponding amplitude can be measured to about one-tenth of the wave-length used for illumination.

In a triple interferometer arrangement which has been recently described[1] the interference pattern formed by reflection from any two parallel surfaces of a quartz plate is compared with the interference patterns formed by reflection from either of these opposing surfaces and an auxiliary fixed surface of glass. With this instrument it is possible to determine the relative displacement of the opposite surfaces. The longitudinal and flexural modes are easily and beautifully differentiated. The instrument is more useful in studying the type of vibration than the simpler interferometer.

There are, however, numerous modes in a rectangular plate which cannot be described to any degree of completeness until the relative motion of any two adjacent surfaces is also known. Fortunately, the triple interferometer arrangement can be simply modified so as to form interference patterns by reflection from two surfaces of the quartz plate which are at right angles as well as from two opposite surfaces. This interferometer, referred to as the "multiple interferometer," combines in a convenient form two optical arrangements, I and II, for determining respectively the relative motion of opposite and adjacent surfaces.

## ARRANGEMENT I

This triple interferometer is shown schematically in Fig. 1. A monochromatic beam of light incident upon the half silvered mirror $A$ is divided into beams $ab$ and $af$. These two beams are in turn divided by the half silvered mirrors $C$ and $H$. The necessary compensating glasses are $B$, $E$ and $G$. $D$ and $I$ are the auxiliary returning mirrors. The quartz plate whose right and left surfaces are under observation is placed at $Q$. $S_1$, $S_2$,

[1] H. Osterberg, J.O.S.A. **23**, 30 (1933).

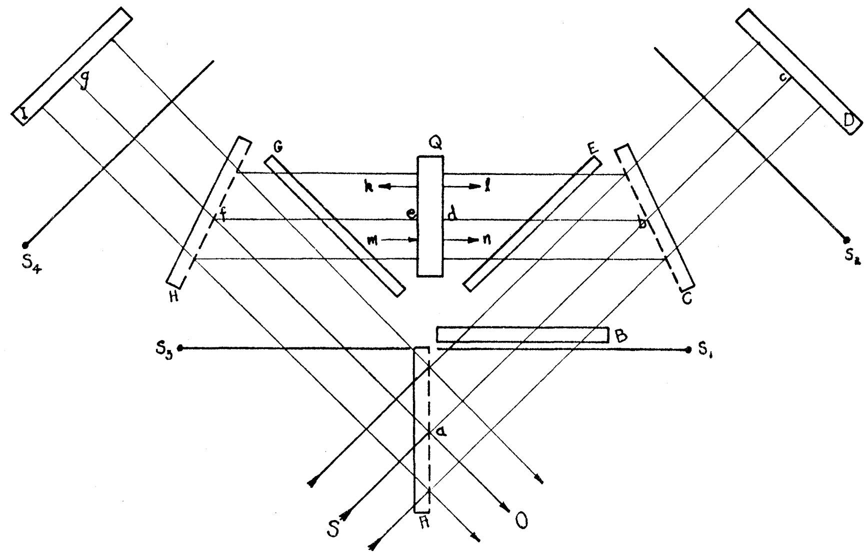


FIG. 1. Schematic diagram of interferometer in arrangement I.

$S_3$ and $S_4$ are shutters which may be operated quickly and smoothly.

When $S_2$ and $S_4$ are closed and $S_3$ and $S_1$ opened, an interference pattern formed by reflection of the beams *abd* and *afe* from the two opposite quartz surfaces is seen by an observer at $O$ provided $A$, $C$, $Q$ and $H$ are properly adjusted. This interferometer will be denoted as I (1). When $S_3$ is closed and $S_1$ and $S_2$ opened, the interference pattern seen at $O$ is formed by the reflection of the beams *bc* and *bd* from the mirror $D$ and the right quartz surface, respectively. This is interferometer I (2). Similarly, when $S_1$ is closed and $S_3$ and $S_4$ opened, the pattern viewed at $O$ is formed by reflection of the beams *fe* and *fg* from the left quartz surface and the mirror I, respectively. This interferometer is called I (3).

Suppose that in the adjustment of I (1) the images of the right and left surfaces of $Q$ are so superimposed that opposing particles on those surfaces are brought into coincidence and consider the differences produced in the fringe disturbances of I (1), I (2) and I (3) by two steps of vibration one of which causes the opposing particles to move as indicated by the arrows $l$ and $k$ and the other of which causes these particles to move as indicated by $n$ and $m$. Both optical paths *db* and *ef* are simultaneously shortened by the type of motion described by $l$ and $k$. Consequently, no fringe disturbance is caused in I (1) provided the amplitudes of vibration of the opposing particles are equal. In general, smaller amplitudes of vibration are seen in I (1) for this type of motion than in either I (2) or I (3). On the other hand, I (1) shows greater amplitudes of vibration than either I (2) or I (3) for the type of motion described by the arrows $n$ and $m$. These two types of relative motion are therefore distinguished by a simple comparison of the amplitudes of vibration revealed by the three interferometers. The measurement of amplitudes of vibration with an interferometer has been discussed in an earlier paper.[2]

## ARRANGEMENT II

In this arrangement (Fig. 2) the group consisting of the dividing mirrors $A$, $C$ and $H$, the returning mirrors $D$ and $I$, the compensating glass $B$, and the shutters is left in the same position as in Fig. 1. $H$ and $C$ are rotated into parallelism with $A$. The quartz plate is placed at $Q$ with its two surfaces *pq* and *pr* perpendicular to *bd* and *ef*, respectively.

Interference fringes are formed by the beams reflected from *pq* and *pr* by opening $S_1$ and $S_3$, closing $S_2$ and $S_4$, and adjusting $C$, $Q$ and $H$.

[2] H. Osterberg, J.O.S.A. **22**, 35 (1932).

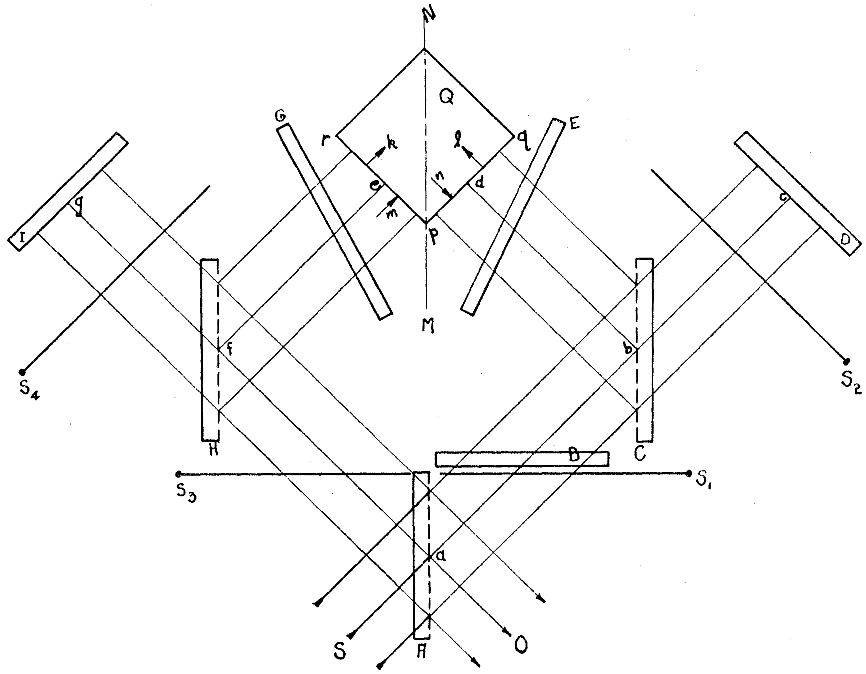


FIG. 2. Schematic diagram of interferometer in arrangement II.

In performing this adjustment $C$ and $H$ are first placed along $bf$ in such a manner that angle $fab$ is approximately a right angle. $Q$ is next arranged such that $bd$ is approximately equal to $ef$ and such that $pq$ is nearly perpendicular to $bd$. The images of $pq$ and $pr$ appear to the observer, $O$, in the direction $afg$. Further adjustments should be made at this point upon $C$, $H$ and $Q$, so that these images stand out clearly and brightly. Various parts of these images may be superposed by tilting $H$ and $C$. In Fig. 2 this is also accomplished by moving either $C$ or $H$ along the line $bf$. When any obstacle containing a pinhole in it is now placed between the source of light, $S$, and $A$, four images of this pinhole are seen by the observer along $afg$. If $A$, $C$ and $H$, have been more than half silvered, the two brightest of these images are those due to reflection from the half silvered surfaces. When these brightest pinhole images are superposed by tilting $Q$, fringes are invariably seen at once provided the differences in the optical paths $abd$ and $afe$ is not too great. Further adjustments may be necessary to improve the appearance of the interference fringes. This interferometer is designated as II (4). Interference fringes between $D$ and $pq$ are next formed by closing $S_3$, opening $S_1$ and $S_2$, and adjusting $D$ alone. In this adjustment the paths $bc$ and $bd$ should first be made approximately equal. The pinhole images may then be superposed as in the preceding case. This interferometer is denoted as II (5). Similarly, by closing $S_1$, opening $S_3$ and $S_4$, and adjusting I alone, interference fringes between I and $pr$ are formed in the interferometer denoted as II (6).

The problem of photographing the above interference patterns is not as simple as might be suspected. A broad, monochromatic source of light and a condensing lens are necessary to secure uniform illumination and fringes with good visibility. A long focus camera is preferable to one of short focal length. In the operation of securing a good image of the interference pattern on the ground glass of the camera it is ordinarily not sufficient to adjust the camera alone. The image on the ground glass can be greatly improved by decreasing or increasing either $abd$ or $afe$. The white light position is not always to be preferred and need not, therefore, be secured. The condition of the half silvered surfaces is much more critical in the photographic work than in that of observing by eye. The evaporation method[3] is highly recommended for half silvering.

The skeleton parts of interferometers II (4), II (5) and II (6), are arranged in Fig. 3, with

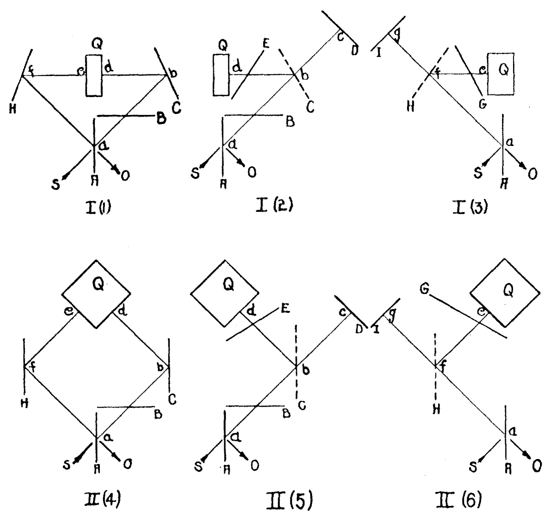


FIG. 3. Skeleton parts of various interferometer arrangements.

those of I (1), I (2) and I (3), to bring out more clearly the essential working parts and differences in these interferometers.

Suppose that in adjusting II (4) the images of *pq* and *pr*, Fig. 2, are superposed in such a way that the particles whose relative motion is indicated by the arrows *l* and *k* are brought into coincidence. For relative motions of the type indicated by *l* and *k*, II (4) will in general indicate smaller amplitudes of vibration than either II (5) or II (6) since in II(4) both optical paths *db* or *ef* are lengthened or shortened simultaneously. On the other hand, for relative motions of the type *n*, *m*, II (4) will always show larger amplitudes of vibration than either II (5) or II (6). The amplitudes in II (4), II (5) and II (6), may be compared in rapid succession with the aid of the shutters.

For descriptions and figures of the mechanical parts of the triple interferometer in Fig. 1, the reader should refer to the earlier paper.[4] The crystal, *Q*, and the dividing mirrors *C* and *H* are mounted upon separate carriage blocks which may be moved on a common track along the line *bdef*. The crystal carriage block was provided with guides by means of which the crystal mounting can be moved along the line *MN*, Fig. 2. These guides are very convenient in shifting from optical arrangement *I* to optical arrangement II. It is necessary only to move the crystal mounting in the direction *MN*, turn the crystal through an angle of 45°, and rotate *H* and *C* into parallelism with *A*.

The multiple interferometer is not limited in application to the rectangular plate. The angle between opposite or adjacent faces may vary quite widely since the beams *bd* and *ef* can be returned to *A* for interference by adjusting the dividing mirrors properly with respect to *Q*.

## Crystal Plates

The multiple interferometer will be illustrated by a group of observations upon two interesting patterns appearing in square plates of *X*-cut. These patterns have previously been studied in both square and circular plates with the aid of a dust and mechanical method by R. B. Wright and D. M. Stuart, who in Fig. 10 of their publication[5] refer to these patterns as *A* and *B*.

The seven square plates are described in Table I in accordance with the terminology suggested by W. G. Cady[6] and followed by the writer.[7] The frequencies of *A* and *B* are listed as

TABLE I.

| Crystal plate | Cut | $x$ (mm) | $y$ (mm) | $z$ (mm) | Direction of electric field | $nA$ | $nB$ |
|---|---|---|---|---|---|---|---|
| 1 | $X$ | 7.867 | 35.984 | 35.979 | X | 66.5 | 83.3 |
| 2 | $X$ | 8.069 | 36.017 | 36.020 | X | 66.25 | 83.2 |
| 3 | $X$ | 4.745 | 36.017 | 36.020 | X | 66.3 | 83.25 |
| 4 | $X$ | 4.745 | 32.108 | 32.113 | X | 74.37 | 93.25 |
| 5 | $X$ | 4.745 | 27.783 | 27.783 | X | 86.24 | 107.5 |
| 6 | $X$ | 4.745 | 27.719 | 27.716 | X | 86.27 | 107.6 |
| 7 | $X$ or $Y$ | 10.381 | 10.382 | 10.385 | X | 209.4 | —— |
| 8 Wright and Stuart | $X$ | 4.810 | 36.02 | 35.98 | X | 66.8 | 83.6 |

Plate 7 is a cube and can therefore be used as an $x$, $y$ or $z$-cut.

[3] C. H. Cartwright and J. Strong, R. S. I. **2**, 189 (1931).

[4] H. Osterberg, J.O.S.A. **23**, 34 (1933).

[5] R. B. Wright and D. M. Stuart, Bur. Standards J. Research **7**, 519 (1931).

[6] W. G. Cady, P.I.R.E. **18**, 2136 (1930).

[7] H. Osterberg, J.O.S.A. **22**, 28 (1932).

$nA$ and $nB$ in kilocycles/sec., and are compared with those observed by Wright and Stuart. These plates have been both cut and plane polished by the writer. Opposite sides are parallel to about 0.001 mm. Adjacent sides are perpendicular to the limit attainable with a good square. The orientation of the plate with respect to its crystallographic axes is accurate to at least one-fourth degree. All plates were cut from the same crystal of Brazilian quartz, which was of good optical quality. Plates 3 to 6 were cut down from plate 2. The crystals were driven by an electric field applied along $X$, the electric axis, through strips connected to the variable condenser of a Hartley oscillator. These strips are often apparent on the photographs. The surfaces under observation were usually silvered.

## Pattern A

Pattern A, which appears at $nA$, the lower frequency, Table I, is described in Fig. 4, with the aid of photographs of the various interference patterns from crystal 6. Corresponding photographs from the other crystals are identical in appearance.

To gain facility in interpreting the interference patterns, the reader should study the mathematical analysis of an earlier paper.[8] It should be borne in mind that when amplitudes of vibration are mentioned throughout the following discussion, these are actually the components of vibration along the normal to the particular surface under observation.

Fig. 4, A, represents the fringe appearance on both major surfaces in interferometers I (2), I (3), II (5) and II (6). The original fringes, almost undisturbed, appear on the corners $a$, $b$, $c$, $d$, which are nearly at rest. The narrow ring of the outer elliptical figure extends over that portion of the major surface whose amplitude is such as to obliterate the original fringes. Within this elliptical ring the amplitude is greater than the above value and reconstructs a set of fringes whose brightness maxima are shifted by one-half fringe width. A continuous increase in the amplitude of vibration results in alternate destruction and reconstruction of the fringes. Each reconstruction is accompanied by a shift of one-half fringe width and results in poorer contrast than in the preceding fringes. A second obliteration surrounds the middle of the major surface. Within this smaller ring of obliteration the greatest amplitudes, sufficient to cause a second reconstruction, are reached.

Fig. 4, F, represents the fringe pattern in I (1) at all amplitudes. No fringe disturbance is seen in this interferometer whereas large fringe disturbances occur in I (2), and I (3). The relative motion of opposing particles on the major surfaces is therefore that indicated by arrows $k$ and $l$, Fig. 1. Pattern A, it appears, is compressional in nature.

Lycopodium powder settled temporarily along the white dotted line at an angle of $-21.4°$ with the optic axis, which is parallel to the edge $db$.

Fig. 4, D, is photographed from the face $db$ in I (2). A node is clearly visible near $b$. The amplitude is very great over a region to the right of $d$ in which it is a maximum. This region can be distinguished at smaller amplitudes of vibration. The pattern from $ac$ in I (3) is so symmetrical with the above pattern that no photograph was taken. It is illustrated by Fig. 4, B, in which the node is present near $c$. In the case of crystal 1 the maximum amplitude of oscillation on $bd$ or $ac$ was sufficient to produce the fifteenth blurring of the fringes. This amplitude is equal to 3.69 wavelengths of the green light used for illumination (5461A). Fig. 4, J, was photographed from I (1) in which the reflecting faces were $bd$ and $ac$. From the presence of the node near the middle of this photograph and a comparison with photographs B and D, one concludes that near the middle of faces $bd$ and $ac$ opposing particles move relatively as indicated by $k$ and $l$, Fig. 1.

The fringe appearance on $ab$ and $dc$ in I (2) and I (3), respectively, is shown in Figs. 4, C and E. These patterns are, again, symmetrical. The nodes occur near the middle of the surfaces. In photographing C the crystal was made to vibrate with less amplitude than in D for the purpose of showing more clearly $m$, the region of greatest amplitude. The pattern Fig. 4, L, was formed in I (1) by reflection from $ab$ and $cd$. Its similarity to Fig. 4, J, is striking. Opposing particles on the middle of $ab$ and $cd$ thus move relatively as indicated by $k$ and $l$, Fig. 1. Since particles in the same surface located on opposite sides of a node move

[8] H. Osterberg, J.O.S.A. **22**, 20 (1932).

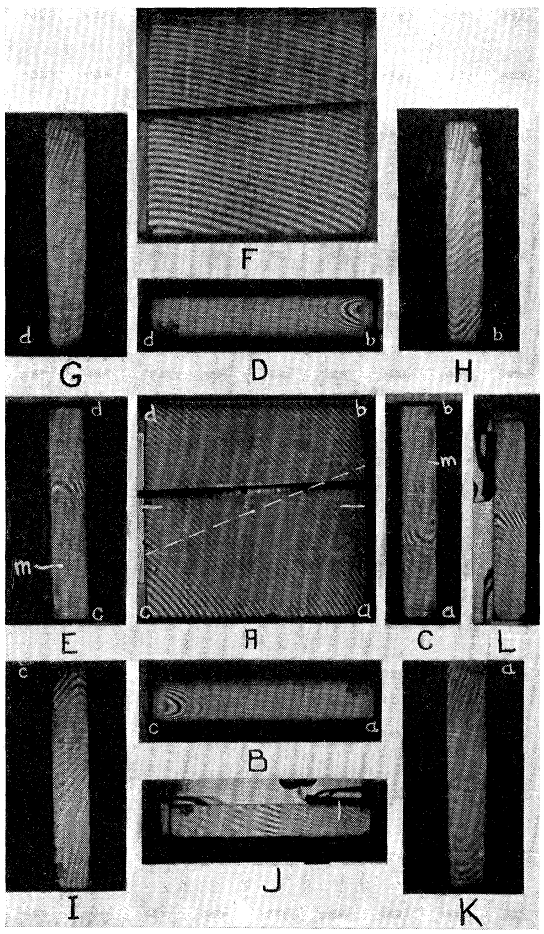


FIG. 4. Photographs of various interference patterns from crystal 6, pattern A.

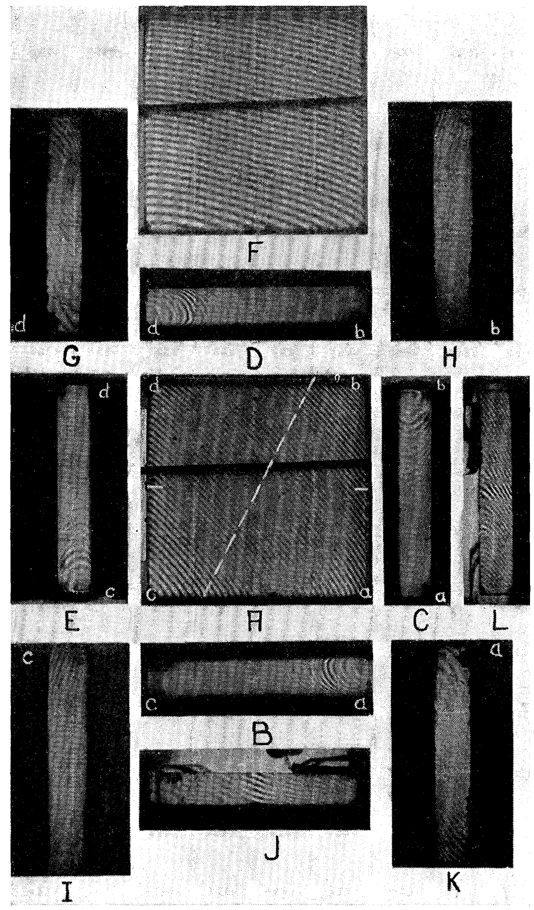


FIG. 5. Photographs of various interference patterns from crystal 6, pattern B.

opposite in direction, it follows that with the simple observations in the above paragraphs the relative direction of motion of the opposite surfaces is known. Figs. 4, G, H, I and K, are formed in II (4) by reflection from two perpendicular faces as in Fig. 2. From Fig. 2 it is clear that in the case of a square plate it is most natural to superpose the images of $r$ and $q$ in adjusting for fringes. In Fig. 4, H, for example, $db$ and $ba$ are the reflecting faces of which the images of $d$ and $a$ are superposed. Corners $b$ of H and $b$ of A correspond. Figs. 4, G, I and K, bear a similar relation to A. One is immediately struck by the similarity of Figs. 4, G, H, I and K. In all cases the middle region suffers the greatest apparent amplitude and the amplitude is more uniform over the surface than in the other photographs. By comparing Figs. 4, C, D and H, it is evident that particles near $a$ and $d$ on the surfaces $ab$ and $db$ are moving relatively as indicated by $k$ and $l$, Fig. 2. The same conclusion applies to the corresponding particles near $a$ and $d$ on the surfaces $cd$ and $ac$ by a similar comparison of Figs. 4, B, E and I. These facts enable one to picture the relative motion of the narrow faces of the crystal.

The relative motion of the two major faces with respect to the edge faces was determined in the following interesting manner. In II (4) an interference pattern very similar to Fig. 4, C was obtained by the superposition of the images of the face $ab$ and a strip extending across the middle of one of the major surfaces, the particular major surface being immaterial since their relative motion was known. The above strip was chosen since the middle part of the major face has the greatest amplitude and since even this amplitude is only about one-fourth of that of the edge faces. In crystal 2, for example, the node on Fig. 4, C, was located at a distance 22.0 mm from $b$. In the above interference pattern this node had suffered an apparent shift to a new position 20.3 mm from $b$. This showed definitely that particles on the major surface move relatively to those near $b$ on $ab$ as indicated by $k$ and $l$, Fig. 2 and relatively to those near $a$ on $ab$ as indicated by $n$ and $m$, Fig. 2.

The nodal lines present on the crystal edge faces, particularly those upon $ab$ and $cd$, become very narrow with increased amplitude of vibration. It is interesting to compare these nodal lines with those of the dust pattern, Fig. 10, a, of the article by Wright and Stuart.[9] One is immediately impressed by the greater certainty and ease with which the optical phenomenon is interpreted. The optical patterns are also subject to being measured with the greater accuracy as, for example, with a long focus travelling microscope. From measurements made in this manner the angle, $\gamma_1$, between the optic axis and a line drawn in the plane of the plate through the nodes on $ab$ and $cd$ was found to be $14°\pm 40'$. A similar line through the nodes on $bd$ and $ac$ makes an angle $\gamma_2 = -52°$ with the optic axis.

The facts established in the preceding paragraphs regarding the type of vibration in pattern A are assembled in Fig. 6. Small arrows have been drawn across the edges to indicate their motion at the instant when the upper major surface is moving toward the reader. This major surface is that which becomes positive upon the application of pressure. The approximate relative amplitude of vibration of the edge faces is given, for example, at some point $C$ by the length $BC$. The displacements along the small arrows appear to be components of two displacements described by the large arrows.

The dust line, $mn$, inclined $\gamma_2 = -21.4°$ with the optic axis cuts the edge faces $ab$ and $cd$ in Fig. 4, A, in the region in which these faces have

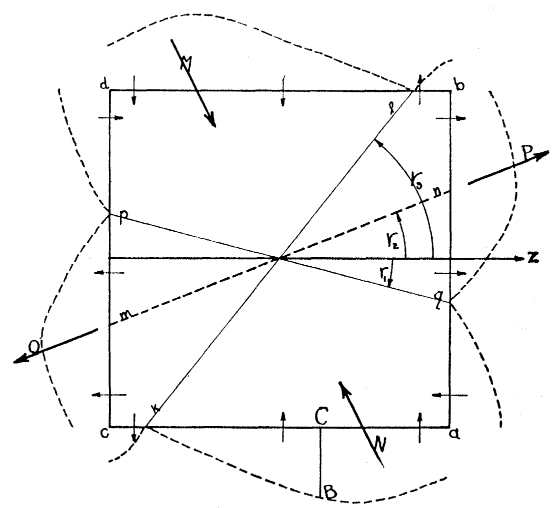


FIG. 6. Summary of facts regarding vibrations in pattern A.

the greatest amplitude. It appears to be a node in the plane of the plate for the compressional vibration along $MN$. The amplitude along $MN$ is somewhat greater than that along $OP$. The above statements are consistent with the observation that lycopodium strewed upon the major surface first moves inward toward $mn$ and outward along it. For consider the actual motion of a particle located within the area $acmn$ in the upper major surface. By neglecting the component parallel to $mn$, this particle is subjected to two simple harmonic motions which are mutually perpendicular and whose phase relations are such that the upward component of motion is accompanied by a larger horizontal component parallel to $N$. The particle thus moves in an elliptical orbit with the proper velocity to impart to the dust particles with which it comes in contact momentum in the direction of $N$, i.e., toward $mn$. Contact with dust particles is made only when the particle is moving upward. Similarly, particles located in the area $bdmn$ in the upper major surface move the dust particles toward $mn$. Particles located along $mn$ in the upper surface are subjected to a horizontal component of vibration only along $mn$. The phase relations between the upward component and the horizontal component along this line is such as to move the dust outward from the center of the plate along the directions $O$ and $P$.

In Fig. 7, following Wright and Stuart, Young's modulus in the plane of an $X$-cut is plotted as

[9] R. B. Wright and D. M. Stuart, Bur. Standards J. Research 7, 519 (1931).

ordinates and $\gamma$, the angle between the optic axis and the direction in which Young's modulus is sought, as abscissas. The line $kl$, Fig. 6, corresponds closely to the direction in which Young's modulus is a maximum. Similarly, $pq$ corresponds closely to the direction in which Young's modulus

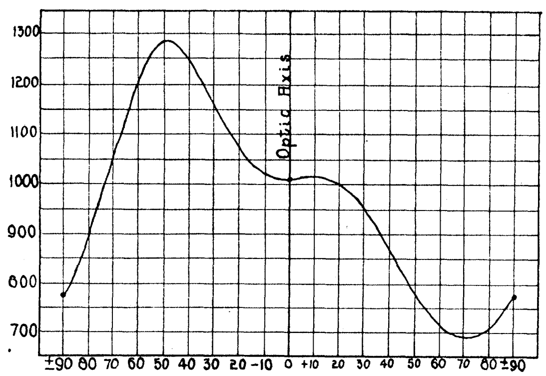


FIG. 7. Young's modulus in the $YZ$ plane of an $X$-cut as given by Wright and Stuart. Young's modulus in kilomegabaryes as ordinates. $\gamma$ in degrees as abscissas.

is a maximum on the other side of the optic axis. The direction $MN$ is that in which Young's modulus is a minimum. Similar relationships regarding the lines through nodes of radial displacement are pointed out by Wright and Stuart in the case of a circular plate of $X$-cut, for which their method of probing the radial air currents can be depended to give quite accurate results.

Pattern A is compressional in nature, formed, without a doubt, by two sets of compressional wave trains propagated in opposite directions in the plane of the plate and incident at angles different from 90° upon the four crystal edges. These angles must be those which enable the wave trains to repeat their course periodically. Under such circumstances the critical values of Young's modulus are of importance in determining the particular form of those patterns for which periodicity is possible. In plates of either $X$ or $Y$-cut the writer has found that one of the most common types of pattern is a regular and beautiful series due to the reflection of flexural wave trains at angles different from 90° upon the four sides of the plate. These flexural wave trains thus "circulate" within the plane of the plate in a manner similar to the compressional waves in pattern A.

## Pattern B

Pattern B is described in Fig. 5, in which the photographs from crystal 6 are arranged as in Fig. 4. The major surfaces show almost the same interference pattern and have the same relative motion in pattern B as in the case of pattern A. This is shown by Figs. 5, A and F. The vibration of the individual edge faces is quite different, as can be judged from Figs. 5, B, C, D and E. Opposite edge faces vibrate symmetrically, as in pattern A. The nodes on $ac$ and $db$ are very distinct. The faces $cd$ and $ab$ could be brought into motion as a whole by increasing the amplitude of vibration, the corners $b$ and $c$ vibrating with less amplitude than $a$ or $d$. Lycopodium powder was found to move toward the dotted white line inclined at $-64°$ with the optic axis and then slide outward as in pattern A. This line cuts $bd$ and $ac$ in those regions where these faces have their greatest amplitude. Figs. 5, J and L, from I (1) indicate that at the middle of the edge faces opposing particles on either set of parallel edge faces move relatively as indicated by $k$ and $l$, Fig. 1 and with equal amplitude. Figs. 5, G, H, K and I, from II (4), are strikingly similar. They show that particles from the middle of any two perpendicular edge faces move relatively as indicated by $m$ and $n$, Fig. 2. These patterns, photographed with the crystal oscillating weakly, possess a more uniform amplitude of oscillation than the others.

In the pattern (not shown) formed in II (4) by reflection from $ac$ and a strip across a major surface, the node present on $ac$ in Fig. 5, B, suffered an apparent shift in the direction $a$ to $c$. This showed that an outward motion of particles on $ac$ located to the left of the node is accompanied by an upward motion of the major surface which faces the reader.

A line in the plane of the plate through the node on $ac$ and on $bd$ forms an angle of $57.5 \pm 1°$ with the optic axis. It does not coincide with any direction in which Young's modulus has any unusual features, Fig. 7.

Fig. 8 is a summary of the main facts regarding pattern B. The small arrows indicate the relative motion of the edges at the instant when the upper major surface is going toward the reader. The approximate relative amplitude at a point $C$ is given in terms of the length $CD$. The dust line, $mn$, forms an angle, $\gamma = -64 \pm 2°$ with the optic axis. The line $pq$ through the nodes on $bd$ and $ac$ forms an angle of $57.5 \pm 1°$ with this axis. Par-

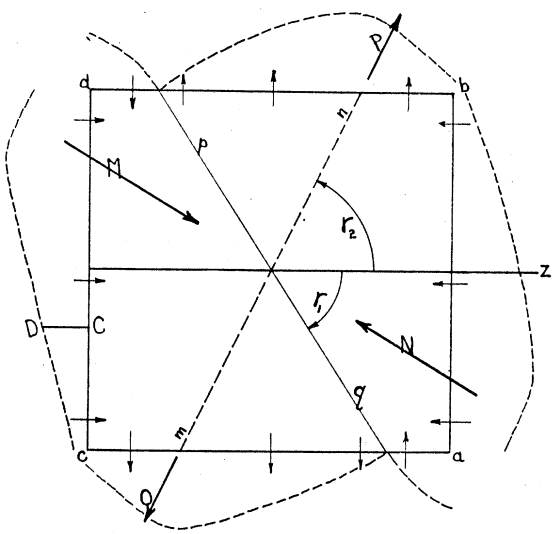


FIG. 8. Summary of facts regarding vibrations in pattern B.

ticles appear to enjoy the maximum displacement in the plane of the plate in the directions $MN$ and $OP$, the larger amplitude being along $MN$. The dust node, $mn$, is most probably the node of vibrations in the plane of the plate along $MN$.

Pattern B, like pattern A, is compressional in nature and formed by two longitudinal wave trains propagated in opposite directions in the plane of the plate. These patterns differ in the very interesting respect that pattern A possesses two sets of radial nodes, determining $kl$ and $pq$ (Fig. 6), while pattern B has only one, determining $pq$, Fig. 8.

## Huyghen's Construction

The publication by Wright and Stuart of Young's modulus for the various directions in quartz plates is of great assistance in the application of Huyghen's construction to determine the relation between the angles of incidence and reflection of a compressional wave incident at any angle upon the boundaries of a quartz plate. The writer has not thus far succeeded, using this method of attack, in discovering which sets of compressional wave trains are those which form either pattern A or B. It is to be expected that though Huyghen's construction will enable one to discover the above wave trains, the actual position of the nodes will also be affected by the phase changes suffered by the waves upon reflection. The calculation of these phase changes for an anisotropic medium as a function of the angle of incidence is a pressing need.

Observations with the interferometer upon a large number of rectangular plates of $X$-cut and one circular plate of this cut have not revealed a single longitudinal pattern due to the reflection of compressional waves back and forth between any two opposite surfaces in the manner in which this phenomenon occurs in an open ended organ pipe. These observations, which apply to waves along $X$, $Y$ or $Z$, are in direct contradiction with conclusions which, in the writer's opinion, have been drawn too freely in the past. The complexity, as regards variation of the amplitude of vibration over the crystal faces, of the mode whose frequency is, supposedly, determined by the thickness of the plate, has occasionally been mentioned.[10, 11] A recent publication by D. W. Dye[12] of some beautiful patterns from vibrating quartz plates contains no example of a pattern in which the two opposite reflecting end surfaces move even approximately as a whole.

It has been stated above that the coincidence of the observed and computed frequencies is a poor criterion for determining the type of vibration. The use of lycopodium powder for this purpose, particularly for plates of small area, is not reliable; for, many patterns which violently remove every trace of the applied powder show a regular set of nodes and antinodes upon this area when viewed simultaneously in the interferometer. The difficulties of interpreting even the simple dust figures of patterns A and B of this report have been discussed above. It is seriously to

---

[10] P. Vigoureux, *Quartz Resonators and Oscillators*, p. 58, 1931.

[11] S. Nishikawa, V. Sakisaka, I. Sumoto, Phys. Rev. **43**, 363 (1933).

[12] D. W. Dye, Proc. Roy. Soc. **A138**, 1 (1932).

be questioned whether it is necessary to carry out the customary method of edge grinding in order to facilitate the excitation of the fundamental longitudinal mode along $X$. By far the greatest number of patterns in the ordinary $X$-cut are due to flexural waves propagated in the plane of the plate. A much smaller number is due to longitudinal waves also propagated in the plane of the plate but incident (as in patterns A and B) at angles different from 90° upon the boundaries of the plate. For a given thickness of plate the effect of edge grinding is thus in general to increase the frequencies of these patterns. It is then a matter of coincidence, persistence, or experience to secure a pattern whose frequency approximates the desired frequency and whose major surfaces possess sufficient polarization for the purpose of frequency control.

It is reasonable to suppose that the fundamental longitudinal mode along the $X$ direction in a quartz plate of $X$-cut cannot be excited (1) unless it is physically possible for a wave front, incident normally upon either of the two parallel reflecting end surfaces to retrace its course after each reflection from the same surface and (2) unless this wave front does not suffer appreciable damping. When these conditions are fulfilled, it then appears that at resonance the converse piezoelectric effect serves primarily as a means of supplying the energy required for sustained oscillations. If Huyghen's construction is used to describe the wave front after reflection, it will be found that the direction of propagation of the infinitesmal portions of the wave front is not parallel with the normal to the wave front. From Fig. 7, it is clear that this direction may form an angle of 40° with the normal, $X$, to the wave front. As a consequence, the wave front after reflection from either of the end faces will have sidled into the edges of the plate and there have suffered reflection before it is incident upon the second end surface. In the case of plates of large $x$ dimension the entire wave front will have sidled into the edges of the plate. For such plates neither condition (1) nor (2) above is satisfied. It should be remembered that this situation differs considerably from the optical one in that the crystal dimensions, and therefore the wavelength, may be large as compared to the wave front.

Young's modulus in quartz assumes its extreme values in the $YZ$ plane, for which Fig. 7, applies. Its maximum value is almost twice as great as its minimum value.

For specially oriented $X$-cuts in which the two reflecting end faces are ground perpendicular to the directions in which Young's modulus is a maximum (or, perhaps, a minimum) the direction of propagation of the infinitesimal portions of the reflected wave front is parallel with the normal to the wave front. For these cases conditions (1) and (2) are satisfied.

This phenomenon, which is fundamental to an understanding of the character of the longitudinal modes possible in an anisotropic solid, is being studied experimentally with some care and will be described in greater detail elsewhere.

## Frequency-Dimensional Ratios of Patterns A and B

The frequencies of patterns A and B are very nearly independent of the thickness, $x$. This is shown in Table I by crystals 1, 2, 3 and 8, whose thicknesses vary, the lengths $y$ or $z$ being constant.

An analysis of the frequencies of crystals 3, 4, 5 and 6, in which the thickness is constant, shows that these frequencies are inversely proportional to the length $y$ or $z$ to an accuracy at least equal to that with which these frequencies can be determined with a General Radio Precision Wavemeter, that is, to an accuracy of about 0.25 percent. These facts are in accord with the supposition that patterns A and B are formed by two compressional wave trains circulating in the plane of the major surfaces.

Pattern A was formed on crystal 7 at 209.4 kc/sec. together with another pattern. The difficulty of keeping these two patterns separate accounts for a mistake in the article[13] on the triple interferometer. In this article crystal 7 is listed as crystal 14. The pattern at 210 kc is incorrectly concluded to be due to a simple longitudinal pattern propagated along $X$ as in an open ended organ pipe, showing, as stated, a peculiar nodal belt on the faces perpendicular to $Y$ and $Z$.

[13] H. Osterberg, J.O.S.A. **23**, 32 (1933).

Pattern A departs widely in this case from the frequency-length proportionality of the preceding paragraph. Its nodes are markedly curved at the smaller amplitudes of oscillation, suggesting end corrections or cross coupling.

Further regrinding of crystal 6 is obviously desirable.

The multiple interferometer is at present, however, being modified to determine the relative motion of all parts of a circular plate. A report on this experiment is forthcoming.

The writer takes pleasure in expressing his indebtedness to the National Research Council for a grant which has been of great assistance in the continuation of this work.

My thanks are also due to J. R. Roebuck for his helpful interest in the progress of this work and his criticism of the manuscript.

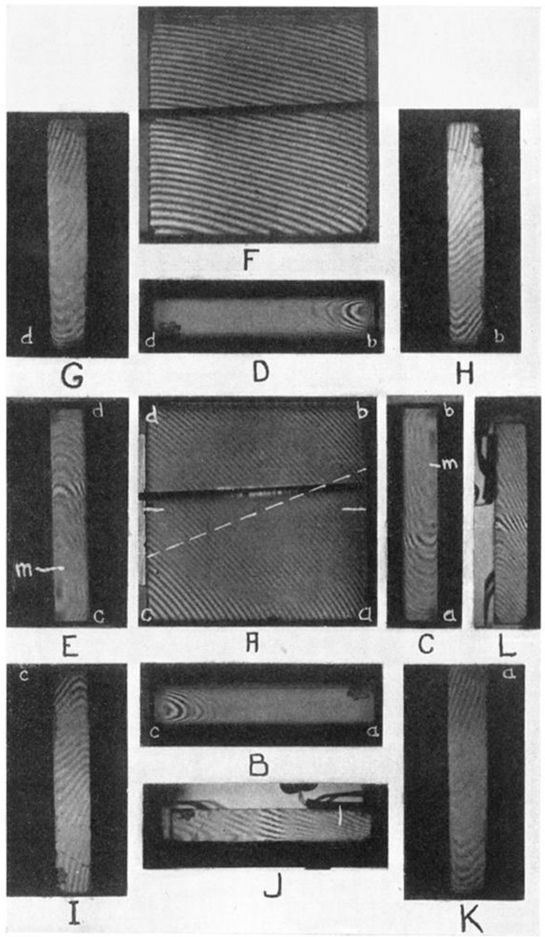


FIG. 4. Photographs of various interference patterns from crystal 6, pattern A.

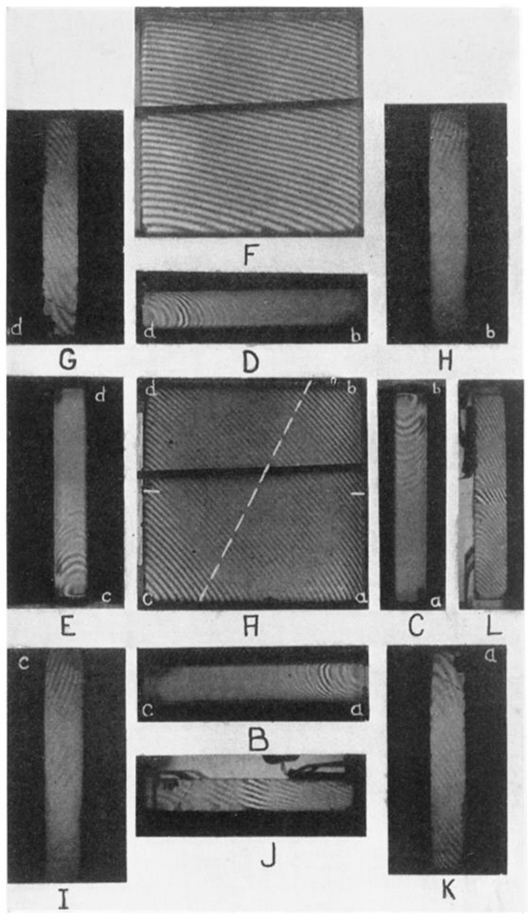


FIG. 5. Photographs of various interference patterns from crystal 6, pattern B.